Advs Exp. Medicine, Biology - Innovations in Cancer Research and Regenerative Medicine (2019) 2: 207–220
https://doi.org/10.1007/5584_2019_343

Published online: 19 June 2019

Evaluation of Proliferation and Osteogenic Differentiation of Human Umbilical Cord-Derived Mesenchymal Stem Cells in Porous Scaffolds

Thuy Thi-Thanh Dao, Chau Thi-Hong Nguyen, Ngoc Bich Vu, Ha Thi-Ngan Le, Phuc Dang-Ngoc Nguyen, and Phuc Van Pham

Abstract

Introduction: Human umbilical cord-derived mesenchymal stem cells (UCMSCs) are multiple potential stem cells that can differentiate into various kinds of functional cells, including adipocytes, osteoblasts, and chondroblasts. Thus, UCMSCs have recently been used in both stem cell therapy and tissue engineering applications to produce various functional tissues. This study aimed to evaluate the proliferation and differentiation of UCMSCs on porous scaffolds.

Methods: UCMSCs were established in a previous study and kept in liquid nitrogen. They were thawed and expanded in vitro to yield enough cells for further experiments. The cells were characterized as having MSC phenotype. They were seeded onto culture medium-treated porous scaffolds or on non-treated porous scaffolds at different densities of UCMSCs (10^5, 2.1×10^5, and 5×10^5 cells/0.005 g scaffold). The existence of UCMSCs on the scaffold was evaluated by nucleic staining using Hoechst 33342 dye, while cell proliferation on the scaffold was determined by MTT assay. Osteogenic differentiation was evaluated by changes in cellular morphology, accumulation of extracellular calcium, and expression of osteoblast-specific genes (including *runx2*, *osteopontin* (*OPN*), and *osteocalcin* (*OCN*)).

Results: The data showed that UCMSCs could attach, proliferate, and differentiate on

Thuy Thi-Thanh Dao and Chau Thi-Hong Nguyen have been contributed equally to this chapter.

T. T.-T. Dao, C. T.-H. Nguyen, H. T.-N. Le, and P. D.-N. Nguyen
Stem Cell Institute, University of Science, VNU-HCM, Ho Chi Minh City, Vietnam
e-mail: thuydao@sci.edu.vn; nthchau225@gmail.com; hale@sci.edu.vn; phucnguyen@sci.edu.vn

N. B. Vu
Stem Cell Institute, University of Science, VNU-HCM, Ho Chi Minh City, Vietnam

Laboratory of Stem cell research and application, University of Science, VNU-HCM, Ho Chi Minh City, Vietnam
e-mail: vbngoc@hcmus.edu.vn; ngocvu@sci.edu.vn

P. Van Pham (✉)
Stem Cell Institute, University of Science, VNU-HCM, Ho Chi Minh City, Vietnam

Laboratory of Stem cell research and application, University of Science, VNU-HCM, Ho Chi Minh City, Vietnam

Department of Animal Physiology and Biotechnology, Biology Faculty, University of Science, VNU-HCM, Ho Chi Minh City, Vietnam
e-mail: phucpham@sci.edu.vn; pvphuc@hcmuns.edu.vn

both treated and non-treated scaffolds but were better on the treated scaffold. At a cell density of 10^5 cells/0.005 g scaffold, the adherent and proliferative abilities of UCMSCs were higher than that of the other densities after 14 days of culture ($p < 0.05$). Adherent UCMSCs on the scaffold could be induced into osteoblasts in the osteogenic medium after 21 days of induction. These cells accumulated calcium in the extracellular matrix that was positive with Alizarin Red staining. They also expressed some genes related to osteoblasts, including *runx2*, *OPN*, and *OCN*.

Conclusion: UCMSCs could adhere, proliferate, and differentiate into osteoblasts on porous scaffolds. Therefore, porous scaffolds (such as Variotis) may be suitable scaffolds for producing bone tissue in combination with UCMSCs.

Keywords
3D porous scaffold · Osteogenic differentiation · UCMSCs · Variotis

Abbreviations

ECM	Extracellular matrix
HAc	Hyaluronic acid
OCN	*Osteocalcin*
OPN	*Osteopontin*
PBS	Phosphate-buffered saline
PFA	Paraformaldehyde
UCMSCs	Umbilical cord-derived mesenchymal stem cells

1 Introduction

Bone tissue is one tissue that is capable of repairing itself through the bone remodeling process (Robling et al. 2006). However, the normal remodeling process is slow and cannot keep up with the repair of excessive damages (David et al. 2007). This leads to an increase of the need for bone graft to treat bone diseases, trauma, and bone cancer (Wang et al. 2014). Although autogenous bone graft is the standard treatment, this method has several limits, including donor site morbidity and constraints on obtainable quantities (Mishra et al. 2016). Allogeneic bone graft is considered to be an alternative treatment method. However, it is hampered by minor immunogenic rejection, disease transmission, and lack of blood supply (Holzmann et al. 2010). Therefore, artificial bone tissue engineering represents a promising therapy to meet the aforementioned unresolved issues. The field of bone tissue engineering has emerged recently as a convenient alternative to facilitate the regenerative ability of host tissues (Amini et al. 2012).

Umbilical cord-derived mesenchymal stem cells (UCMSCs) have been demonstrated to have the capacity to differentiate into multiple cell lineages in all three embryonic germ layers (Wang et al. 2009) and can be harvested at a low cost without an invasive procedure (Chen et al. 2013). Moreover, several reports have indicated that human UCMSCs exhibit potential of osteogenic differentiation on three-dimensional scaffolds (Wang et al. 2010; Ahmadi et al. 2017). Osteogenic differentiation of MSCs takes place at different stages, with each stage characterized by the expression of specific genes (Bruderer et al. 2014). In the early stages, there is a strong proliferation of cells. Then, the growth tends to decrease as the differentiation process begins (Cooper 2000).

There are many vital transcription factors for osteoblast differentiation. Among of them, *runx2* is a main determinant of osteoblast differentiation and controls bone formation (Wang et al. 2010; Fakhry et al. 2013). *Runx2* belongs to the *runx* family of transcription factors and regulates osteoblast differentiation (Ziros et al. 2008). It is strongly expressed in the early stages of osteoblast differentiation, particularly in the first week of differentiation (Fakhry et al. 2013). The expression of *runx2* leads to the upregulation of crucial genes in the osteoblast differentiation, such as *osteocalcin*, *alkaline phosphatase*, *bone sialoprotein*, and *osteopontin* (Ducy et al. 1997). *Osteocalcin* (*OCN*) constitutes 1–2% of the matrix proteins and is the most abundant non-collagenous protein that is exclusively secreted by osteoblasts (Lian et al. 1989). *OCN*

controls the size and speed of bone formation (Roach 1994). *Osteopontin* (*OPN*) is another important non-collagenous protein in the bone matrix that is involved in bone remodeling (McKee and Nanci 1996). *OPN* contains the Arg-Gly-Asp sequence as the cell-binding motif; this motif links the adhesion molecules of cells to the extracellular matrix in the mineralized bone matrix (Roach 1994; Oldberg et al. 1986). *OCN* and *OPN* are expressed in mature osteoblasts only and are absent at the early stages; thus, they are markers of late osteoblast differentiation (Wang et al. 2010; Rutkovskiy et al. 2016). In short, the expression of these genes indicates that MSCs have differentiated into osteoblasts.

There are various scaffolds that have been used in bone engineering including natural polymers scaffolds, such as collagen (Aravamudhan et al. 2013), chitosan (Costa-Pinto et al. 2011), silk fibroin (Vepari and Kaplan 2007), and hyaluronic acid (HAc) (Pavasant et al. 1994). Synthetic polymers scaffolds like polyesters (e.g., polyglycolic acid, polylactic acid, polycaprolactone) are the most commonly used as copolymers. Compared to these scaffolds, the Variotis scaffold (Biometic, Sydney, Australia) is a novel scaffold that is comprised of a highly interconnected and porous structure (> 95%). Based on the unique pore structure, the Variotis scaffold is a suitable scaffold for both soft and hard tissue regeneration applications. The scaffold is made from a polyester-based material that is used to enhance cell attachment and proliferation (Zhang et al. 2013). Previously, the scaffold was used to repair cartilage lesion and heal wounds (Ark et al. 2016; Zhang et al. 2015). To date, the Variotis scaffold shows potential for applications that promote cell growth, as well as vascular and extracellular matrix (ECM) formation. Therefore, it is a promising scaffold for tissue engineering (Zhang et al. 2013).

In this study, we aimed to investigate the adherence and proliferation of UCMSCs on the porous scaffold. Morphological changes, calcium extracellular deposition, and specific gene expression were also surveyed after osteogenic differentiation.

2 Materials-Methods

2.1 Porous Scaffold

Porous scaffolds (Variotis, Biometic, Sydney, Australia) with a pore size in excess of 100 μm were weighed using a balance to reach 0.005 g. The scaffolds samples were divided randomly into two groups: treated and non-treated. For the pretreated group, scaffold samples were immersed in culture medium for 24 h.

2.2 Characteristics of Human Umbilical Cord Mesenchymal Stem Cells

The UCMSCs were isolated per previously published and cryopreserved (Van Pham et al. 2016). The cryopreserved UCMSCs were thawed following the protocol of Pham Van Phuc et al. (Van Pham et al. 2016). Briefly, the vials were placed in a water bath at 37 °C for 1–2 min, and then thawing medium was added and centrifuged at 100 g for 5 min to collect the cell pellet. The pellet was resuspended with 3 mL MSCCult medium (Regenmedlab, Ho Chi Minh City, Vietnam) and cultured in a T-25 flask in an incubator at 37 °C, 5% CO_2.

UCMSCs were characterized as mesenchymal stem cells based on the minimal criteria of MSCs, as suggested by the International Society for Cellular Therapy (ISCT), which includes cellular morphology, marker profiles, and differentiation potential. For marker profiles, the expression of certain markers of UCMSCs was evaluated by flow cytometry per published protocol (Van Pham et al. 2016). Briefly, UCMSCs were suspended in staining buffer at 10^4 cells/100 µl in a tube. Then, each tube was stained with specific antibodies, such as CD14-FITC (Santa Cruz Biotechnology, Dallas, Texas), CD34-FITC (Santa Cruz Biotechnology), CD73-FITC (Santa Cruz Biotechnology), CD90-FITC (Santa Cruz Biotechnology), CD44-APC (Sigma), and HLA-DR-FITC (BD Biosciences) for 30 min in the

dark at room temperature. Stained cells were washed with PBS twice to remove the extra antibodies, and then analysis of marker expression was conducted using an FACSCalibur instrument (BD Biosciences, Franklin Lakes, New Jersey) and compared to unstained and isotype controls.

For in vitro differentiation, UCMSCs were induced to several kinds of mesoderm cells, including adipocytes, osteoblasts, and chondroblasts, in the inducing medium (StemPro™ Adipogenesis Differentiation Kit, StemPro™ Osteogenesis Differentiation Kit, StemPro™ Chondrogenesis Differentiation Kit, all bought from Thermo Fisher Scientific, Waltham, MA). For adipocyte differentiation, after 14 days of induction, the medium was removed, and cells were washed with phosphate-buffered saline (PBS) and fixed in paraformaldehyde (PFA), 4% for 1 h. The cells were washed again with PBS and stained with Oil Red dye (Sigma-Aldrich, Louis St., MO). For chondroblast differentiation, after 21 days of induction, cells were also washed with PBS and stained with Alcian Blue (Sigma-Aldrich, Louis St., MO) to detect proteoglycan deposition. For osteoblast differentiation, after 21 days of induction, cells were washed twice with PBS and then stained with Alizarin Red dye (Sigma-Aldrich, Louis St., MO) to detect accumulation of extracellular calcium.

2.3 Seeding UCMSCs onto Porous Scaffold

UCMSCs were expanded in the flask until they reached approximately 80% confluency. They were then dissociated with trypsin/EDTA, 0.25% (Sigma-Aldrich, Louis St., MO). UCMSCs were suspended in culture medium at different cell densities (10^5, 2×10^5 and 5×10^5 cells, per 0.005 g scaffold). Cell suspensions were directly seeded onto the two groups of scaffolds: pretreated and un-pretreated scaffolds (in 15 ml Falcons). Then, the cell-seeded scaffolds were cultured at 37 °C, 5% CO_2.

2.4 Evaluation of Cell Proliferation on the Scaffold

Cell proliferation was evaluated on the scaffold by observation under a microscope and by MTT assay. UCMSCs on scaffolds were observed after 3, 7, 14, and 21 days of seeding, via a microscope. Proliferation of the cells was assessed by MTT assay at 3, 7, and 14 days. For all assays, non-seeded scaffolds were used as a negative control.

In the MTT assay, culture medium was removed. Then, 500 μl fresh medium and 50 μl MTT reagent (5 mg/ml) were added into each well. The samples were incubated at 37 °C for 4 h. MTT-containing medium was replaced by 500 μL DMSO solution (Sigma-Aldrich, Louis St., MO). The samples were vortexed, and the absorbance at 595 nm was recorded by a DTX-880 system (Beckman Coulter, Brea, CA).

2.5 Osteogenic Differentiation of Seeded Scaffolds

Seeded scaffolds were cultured for 14 days to expand the UCMSCs on the surface. Then, the culture medium was replaced by the osteogenic medium (StemPro™ Osteogenesis Differentiation Kit, Thermo Fisher Scientific, Waltham, MA) for 28 days and refreshed with osteogenic medium every 4 days. The osteogenic differentiation of UCMSCs on the scaffolds was evaluated based on (1) morphology, (2) deposition of extracellular calcium, and (3) osteoblast-specific gene expression.

Changes in cellular morphology were observed after 7, 14, 21, and 28 days of induction. After 21 and 28 days of induction, cell-seeded scaffolds were stained with Alizarin Red dye to detect deposition of extracellular calcium.

The expression of certain genes related to osteoblasts was investigated; these included *Runx2*, *OCN*, *OPN*, and *β-actin*, at four time points after induction (7, 14, 21, and 28 days). UCMSCs on scaffolds in both groups were detached by Detachment solution (Regenmedlab,

Table 1 Primer sequences of the specific genes for osteogenic differentiation

Gene	Primer sequence (5′ to 3′)		T_m (°C)	Product size (bp)	GenBank no.
β-Actin	Forward	AGAGCTACGAGCTGCCTGAC	54,5	184	NM_001101.4
	Reverse	AGCACTGTGTTGGCGTACAG			
OCN	Forward	GTGACGAGTTGGCTGACC	53,3	114	NM_1991735
	Reverse	TGGAGAGGAGCAGAACTGG			
OPN	Forward	GACACATATGATGGCCGAGGTGATAG	59	111	NM_001251830.1
	Reverse	GGTGATGTCCTCGTCTGTAGCATC			
Runx2	Forward	GGAGTGGACGAGGCAAGAGTTT	54,5	133	NM_001278478.1
	Reverse	AGCTTCTGTCTGTGCCTTCTGG			

HCM City, Vietnam). The cell pellets were used to isolate total RNA by easy-BLUE Total RNA Extraction Kit (iNtRON) following the manufacturer's instructions. Quantitative real-time PCR was performed using 2x qPCRBIO SyGreen 1-Step Lo-ROX (PCRBIO System, London, United Kingdom) using gene-specific primers (Table 1). The amplification cycle included 15 min of reverse transcription at 45 °C, 2 min of polymerase activation at 95 °C, 40 cycles of amplification for all genes with 5 s of denaturation at 95 °C, and 15 s of annealing at the temperature suitable for each gene.

2.6 Statistical Analysis

All data were expressed as mean ± SD and analyzed by GraphPad Prism software (GraphPad Prism Inc., San Diego, CA). Statistical significance was determined by a statistical threshold of $p < 0.05$.

3 Results

3.1 UCMSCs Exhibited MSC Phenotype

UCMSCs exhibited certain characteristics of mesenchymal stem cells, as suggested by the International Society for Cellular Therapy (ISCT). These included display of fibroblast-like shape when adhering on a plastic surface (Fig. 1a), successful differentiation into adipocytes which were positive with Oil Red dye staining (Fig. 1b), differentiation into osteoblasts which were positive with Alizarin Red (Fig. 2c), and differentiation into chondroblasts which were positive with Alcian Blue (Fig. 1d). They also displayed the MSC immunophenotype, including being positive for CD44 (99.02%), CD73 (95.05%), and CD90 (91.98%) (Fig. 1k–m) and being negative for HLA-DR (0.68%), CD14 (5.76%), and CD34 (5.15%) (Fig. 1h–j).

3.2 Adherence of UCMSCs on Treated and Non-treated Porous Scaffolds

Under microscopy, adhesion of UCMSCs increased on both the non-treated and treated scaffolds during culturing. On the non-treated scaffolds, UCMSCs attached and formed cellular clusters (Fig. 2a). The cellular clusters were gradually bigger and spread out on the 7th day (Fig. 2b). After 14 days of culture, the growth of UCMSCs increased and created links with structured fibers. The cell plaques were clearly observed (Fig. 2c). On day 21, the plaques were significantly larger than the previous days (Fig. 2d).

On the treated scaffolds, after 3 days of culture, UCMSCs attached on the scaffolds to form large cell plaques. These cell plaques grew rapidly and became larger on the 7th and 14th day (Fig. 2f–g), and the fibers of the scaffolds were completely linked together. On the 21st day, the cell plaques were observed to be thicker than the previous days (Fig. 2h).

UCMSCs (on scaffolds) which stained blue from nuclei staining with Hoechst 33342 stain

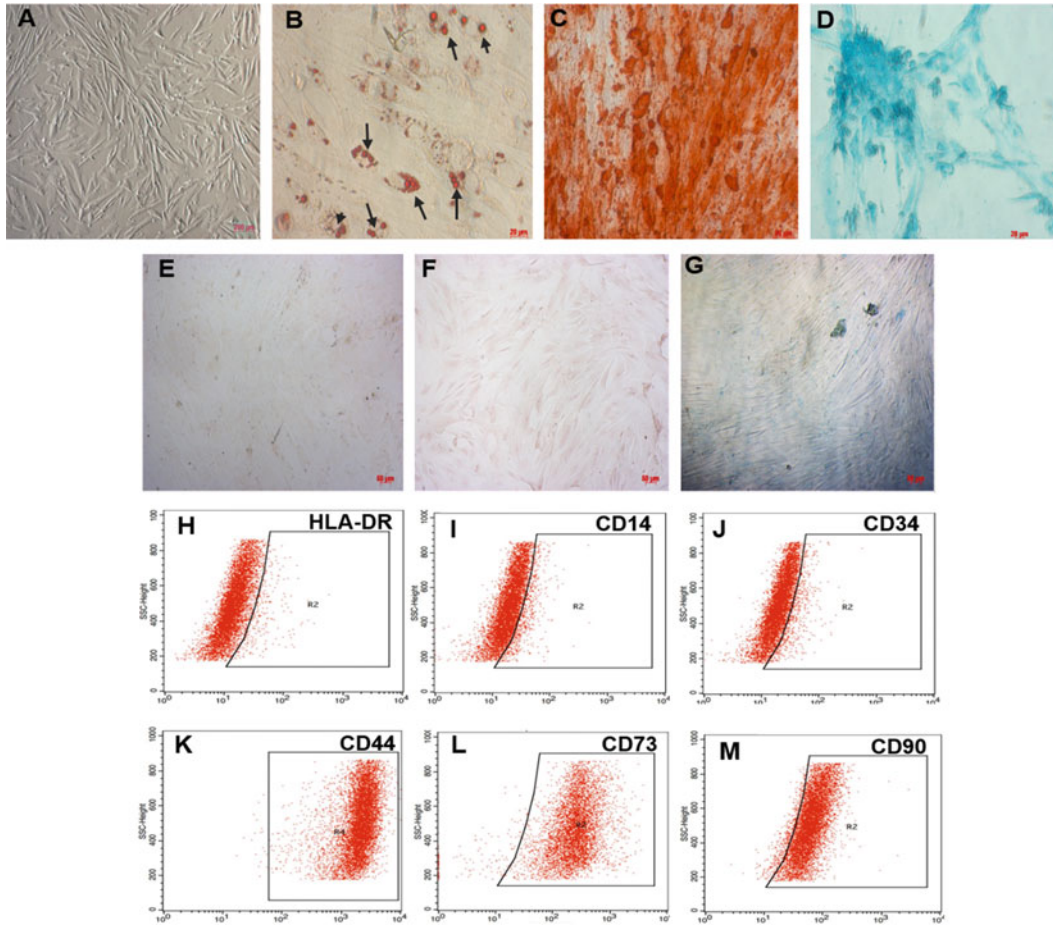

Fig. 1 UCMSC phenotype. UCMSCs express the characteristics of mesenchymal stem cells: fibroblast-like morphology (**a**), accumulation of lipids (**b**), extracellular calcium (**c**), and proteoglycans (**d**), as detected by Oil Red, Alizarin Red, and Alcian Blue after induction; the controls were negative with these dyes (**e, f, g**). The results of flow cytometry showed lack expression of HLA-DR (**h**), CD14 (**i**), and CD34 (**j**) and positive expression of CD44 (**k**), CD73 (**l**), and CD90 (**m**)

were observed via fluorescent microscopy (Fig. 3). The results showed that UCMSCs could attach on the surfaces and pores of scaffolds. It was observed that fewer cells attached on the non-treated scaffolds than on the treated scaffolds. This indicated that UCMSCs attached on the surface of the treated scaffolds to a greater extent. Cell counting showed that the number of cells that attached on the treated scaffolds was significantly higher than the non-treated scaffolds by 1.33 ± 0.12-fold ($p < 0.05$) after 7 days of culture (Fig. 4).

All above results demonstrated that the adhesion of UCMSCs on the treated scaffolds was better than on the non-treated scaffolds. Therefore, treated scaffolds were used in subsequent experiments.

3.3 UCMSC Proliferation on Pretreated Porous Scaffold

After 3 days of culture, UCMSCs attached on the pretreated scaffold. At a density of 10^5 cells/

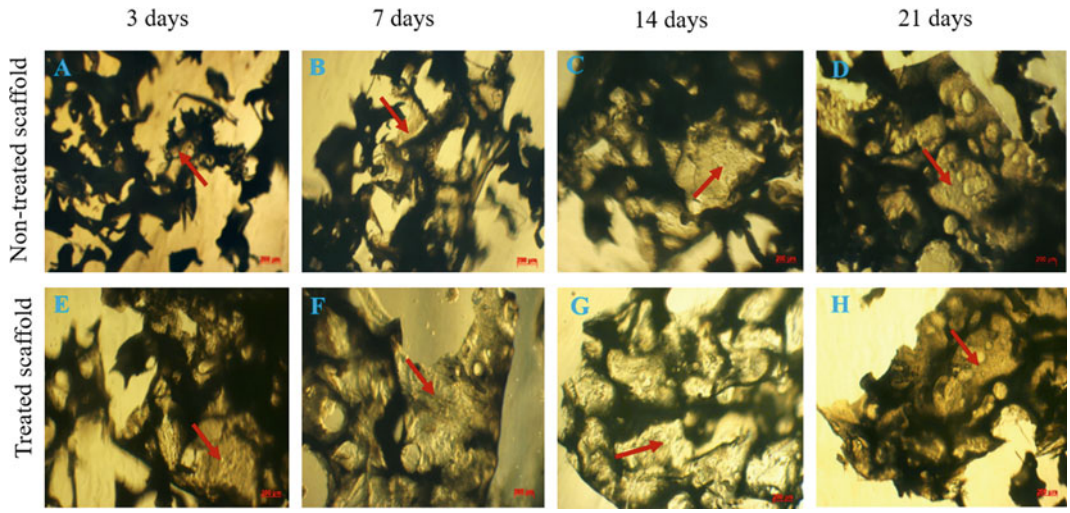

Fig. 2 The adhesion of UCMSCs on the Variotis scaffold. UCMSCs on non-treated scaffold after culture for 3 days (**a**), 7 days (**b**), 14 days (**c**), and 21 days (**d**); UCMSCs on treated scaffold after culture for 3 days (**e**), 7 days (**f**), 14 days (**g**), and 21 days (**H**)

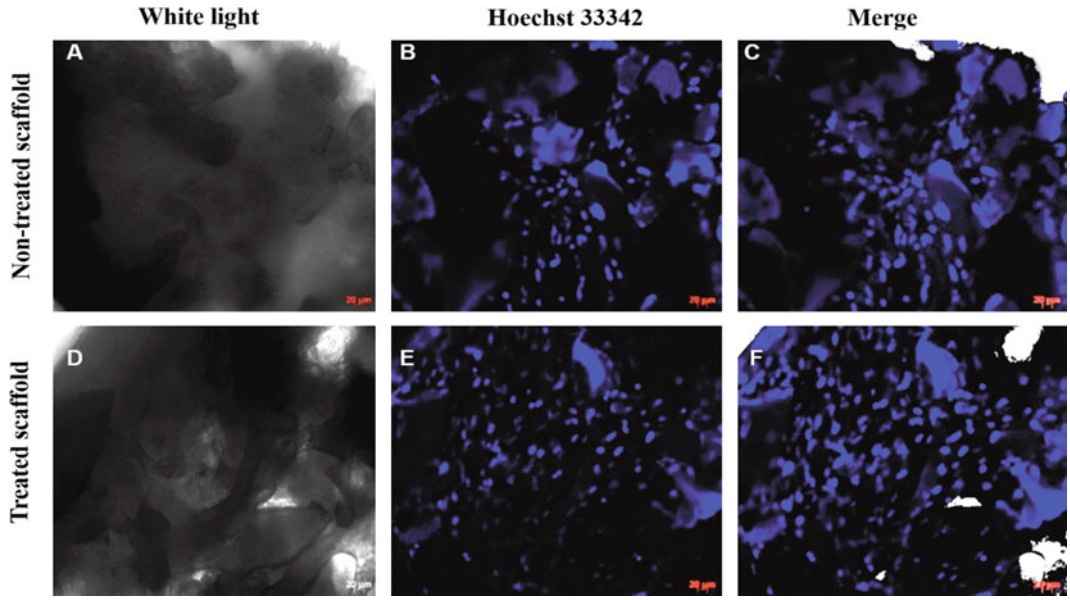

Fig. 3 Cell adhesion observed using Hoechst 33342 after culturing for 7 days. The non-treated scaffold with cells observed under white light (**a**), or fluorescent light (**b**), and the merged image of white light and fluorescent light (**c**). The treated scaffold with cells under white light (**d**), or fluorescent light **(e)**, and the merged image of white light and fluorescent light (**f**)

0.005 g scaffold (Fig. 5a), the cells formed clusters, while at the density of 2×10^5 cells/0.005 g scaffold, the cells spread out to create small plaques (Fig. 5e). At the 7th day, these cells consecutively grew and filled out on all scaffolds (Fig. 5b, f). The cell plaques were bigger and distinctly defined after 14 and 21 days (Fig. 5c, d, g, h). Meanwhile, at a density of

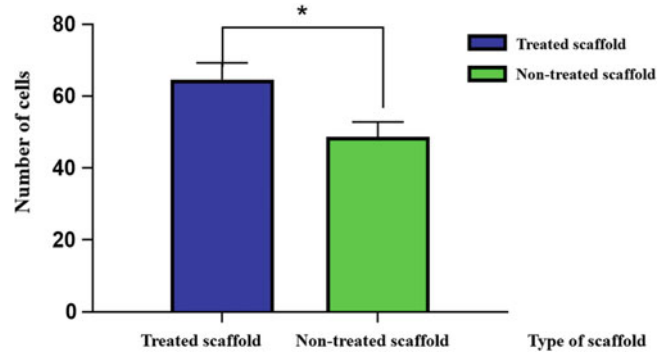

Fig. 4 The number of cells on pretreated and non-pretreated scaffolds. The count of UCMSCs on the treated scaffold was greater than on non-treated scaffold after culture for 7 days; (∗): $p < 0.05$

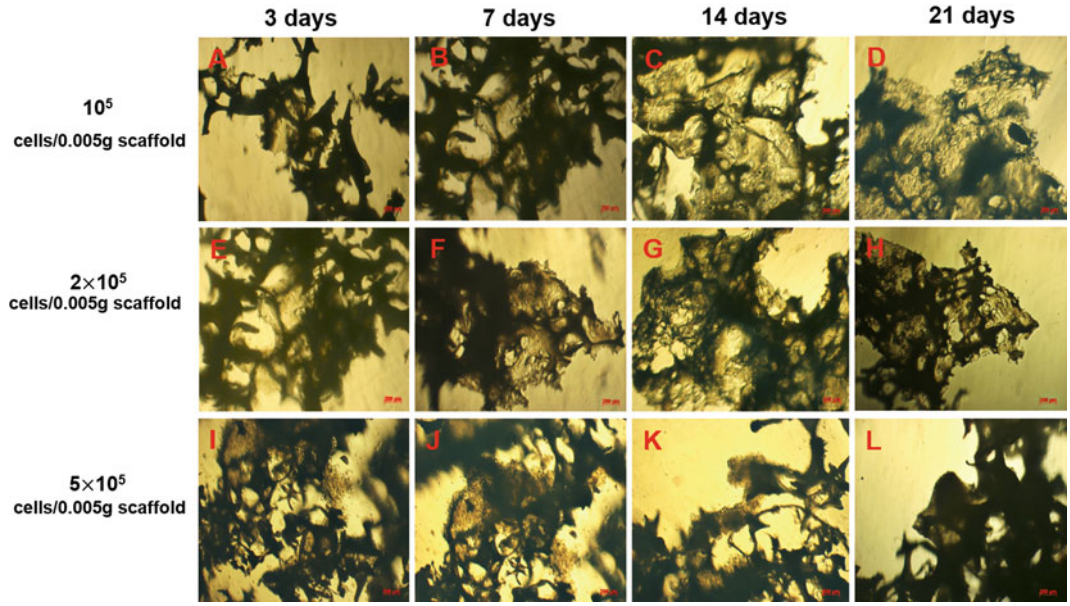

Fig. 5 The cells were seeded on the scaffold at different densities. Cells at a density of 10^5 cells/5 mg scaffold after culturing for 3 days (**a**), 7 days (**b**), 14 days (**c**), and 21 days (**d**). Cells at a density of 2×10^5 cells/5 mg scaffold after culturing for 3 days (**e**), 7 days (**f**), 14 days (**g**), and 21 days (**h**). Cells at a density of 5×10^5 cells/5 mg scaffold after culturing for 3 days (**i**), 7 days (**j**), 14 days (**k**), and 21 days (**l**)

5×10^5 cells/0.005 g scaffold, UCMSCs tended to cluster together before adhering on the scaffolds (Fig. 5i). The cell cluster was loosely connected and could not enter inside these scaffolds (Fig. 5j, k). At the 21st day, the clusters were no longer attached on the scaffolds and were removed after replacement with fresh medium (Fig. 5l).

To evaluate cell expansion on the scaffold, we used the MTT assay to measure cellular proliferation of the various seeded cell densities on the pretreated porous scaffold. It was generally noted that the OD index of MTT assay indicated growth of UCMSCs on the pretreated scaffolds after seeding up to day 14. However, the results in Fig. 6 showed that proliferation rates of UCMSCs of the various cell densities were different (Fig. 6).

At the 3rd day of culture, the proliferation rate of UCMSCs seeded at a density of 10^5 cells/

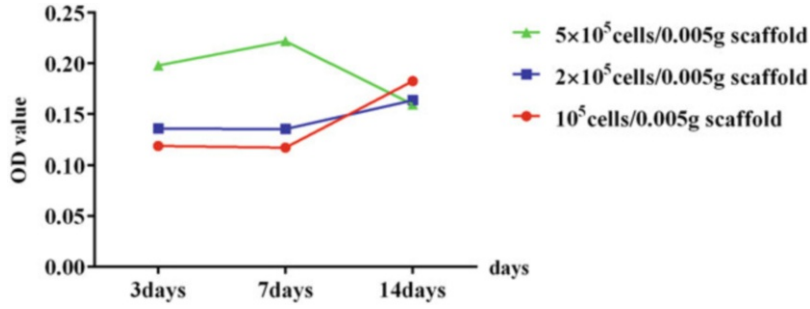

Fig. 6 Cell proliferation measured by MTT assay. UCMSCs slowly grew after 7 days of seeding with 1×10^5 and 2×10^5 cells/0.005 g scaffold, while strong proliferation was recorded for the density of 5×10^5 cells/0.005 g scaffold. However, cell growth was significantly reduced at day 14; on this day, the increase of cell proliferation was found for the other cell densities

0.005 g scaffold was slower than the other groups (2×10^5 and 5×10^5 cells/0.005 g scaffold). For 5×10^5 cells/0.005 g scaffold density, at the day 7th of culture, the proliferation rate was highest and was 1.13 ± 0.08-fold greater compared to that at day 3 ($p < 0.05$) for this group. The cell proliferation rate at day 14 was significantly reduced compared to day 7 and lower than that at day 3 of culture. For the other densities (10^5 and 2×10^5 cells/0.005 g scaffold), the proliferation seemed stable from day 3 to day 7 of culture. However, at the 14th day, these cells considerably expanded and achieved a higher concentration than that at day 7; there was a 1.33 ± 0.003-fold and a 1.13 ± 0.04-fold ($p < 0.05$) increase in the densities of 10^5/0.005 g scaffold and 2×10^5 cells/0.005 g scaffold, respectively. These results demonstrated that the density of 10^5 cells/0.005 g scaffold induced robust cell expansion on pretreated porous scaffolds after 14 days of culture. Thus, this density was used for subsequent experiments.

3.4 Osteogenic Differentiation of UCMSCs on the Scaffold

3.4.1 Change in Morphology

After 7 and 14 days of induction (in the differentiation medium) of 10^5 cells/0.005 g scaffold on pretreated porous scaffolds, the morphology of UCMSC population showed no negligible change (Fig. 7b, c) compared with those in the controls (no induction and culture in culture medium). However, at 21 days of differentiation, these cells condensed together and attached on the fibers of the scaffold (Fig. 7d). Condensation was clearly observed on the 28th day of induction (Fig. 7e), while UCMSCs consecutively spread and filled out the scaffold after 42 days of culturing (Fig. 7f).

3.4.2 Accumulation of Extracellular Ca^{2+}

After 21 and 28 days of osteogenic differentiation, cells on the scaffold became positive with Alizarin Red, and the color was stronger at day 28 (Fig. 8). However, the deposition of Ca^{2+} was not detected in the control sample (undifferentiated). The result of staining with Alizarin Red showed that there was an accumulation of extracellular calcium.

3.4.3 The Expression of Osteogenic Genes

During induction, the osteogenic genes changed upon investigation. *Runx2* was known as a transcriptional factor to activate osteogenesis. Our results showed that the expression of *runx2* was upregulated compared to control group (undifferentiated) (Fig. 9). After 7 days of induction, the expression of *runx2* was stronger and higher than non-induced cells by 2.5 ± 0.45-fold ($p < 0.05$).

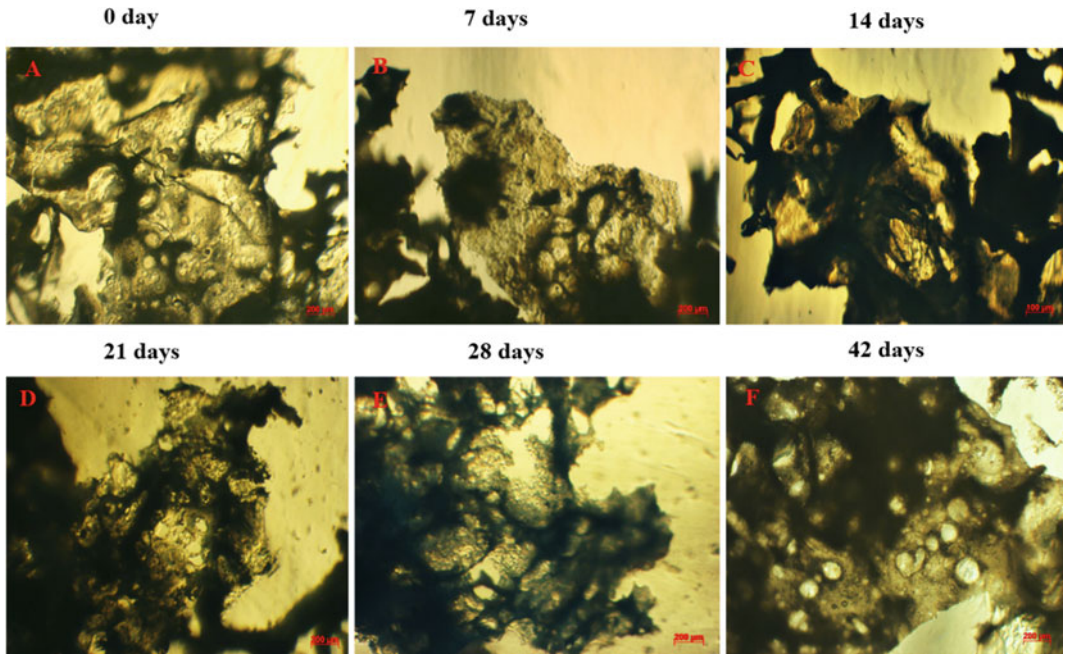

Fig. 7 The shape of UCMSCs in the osteogenic medium. Non-differentiated cells (**a**), differentiated on scaffold for 7 days (**b**), 14 days (**c**), 21 days (**d**), 28 days (**e**), and 42 days (**f**)

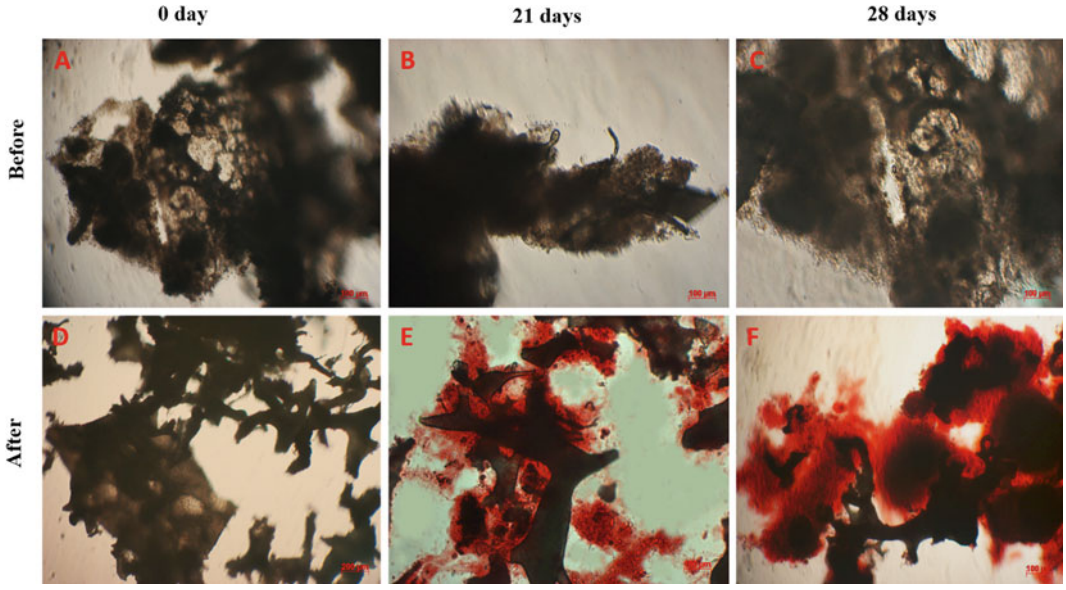

Fig. 8 Results of Alizarin Red staining on UCMSCs. Cells were cultured in normal growth medium (**a**), in osteogenic medium after 21 days (**b**), and for 28 days before dying (**c**). Cells were cultured in normal growth medium (**d**), or osteogenic medium after 21 days (**e**), or osteogenic medicine after 28 days (**f**)

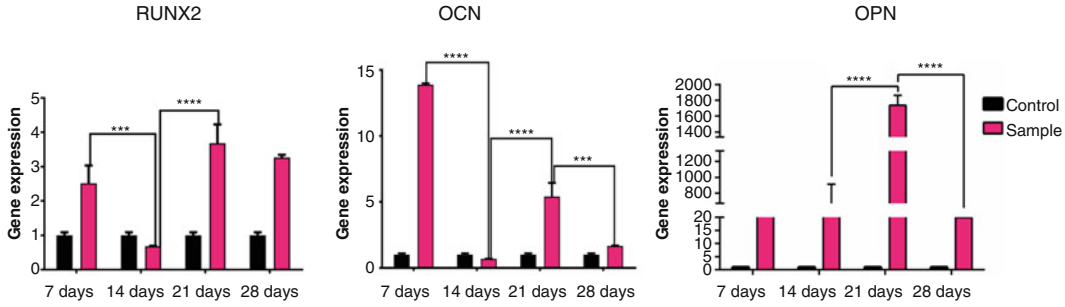

Fig. 9 Gene expression during osteogenic differentiation. Osteogenesis-associated genes, such as *runx2*, *OCN*, and *OPN*, were enhanced during induction, compared to the control group, particularly at the 21st day; (∗): $p < 0.05$

However, this expression significantly decreased at day 14 of differentiation and was lower than that for cells in the control group by 0.68 ± 0.06-fold and lower than them at the 7th day of differentiation by 3.7 ± 0.63-fold. On the 21st day, the expression of *runx2* in induced group was enhanced and reached the maximum and was higher than them in the 7th day by 1.46 ± 0.25-fold ($p < 0.05$). After 28 days of induction, *runx2* was negligibly decreased compared to the 21st culture day; however, that value was still higher than the control group by 3.26 ± 0.2-fold.

The expression profile of *runx2* correlated with *OCN* profile. The expression of *OCN* was upregulated to the highest level by 13.9 ± 1.69-fold compared to the control group on the 7th day of induction. On the 14th day, *OCN* expression sharply decreased compared to the 7th day and to control (20.2 ± 0.08-fold and 0.69 ± 0.06-fold, respectively). However, on the 21st day, the *OCN* expression increased by 7.85 ± 1.42-fold compared to the 14th day and was 5.4 ± 1.46-fold greater than the control group (non-induced). On the 28th day, the expression of *OCN* decreased and was lower by 3.24 ± 0.61-fold than that at day 21; meanwhile, the expression was higher than non-differentiated cells by 1.66 ± 0.14-fold.

Moreover, *OPN* gene expression increased from day 7 to day 21 and was higher than the control group. On the 7th day, the expression of OPN was stronger than that of the non-differentiated ($p < 0.05$). On the 14th day, the expression of *OPN* increased by 2.25 ± 0.65-fold compared with the 7th day and reached the highest level on the 21st day. However, the expression was considerably reduced after 28 days of induction.

4 Discussion

Bone tissues are widely used in bone grafting to treat bone diseases, trauma, and bone cancer. This study aimed to investigate the expansion and differentiation of UCMSCs on porous scaffolds to develop in vitro-engineered bone tissues for clinical applications.

In the first experiment, we expanded and characterized the UCMSCs. According to the International Society for Cellular Therapy (Dominici et al. 2006), human mesenchymal stem cells should be defined by adherence on culture surface, expression of specific markers (CD73, CD90, and CD105; lack of CD14, CD34, CD45 or CD11b, CD79 alpha or CD19, and HLA-DR), and differentiation capacity into adipocytes, osteoblasts, and chondrocytes in vitro. The results from our study showed that UCMSCs, after thawing, retained the characteristics of mesenchymal stem cells.

Indeed, in this study, we also compared the proliferation rate of UCMSCS on both pretreated and non-pretreated scaffolds. The results showed that the pretreated scaffold showed significant results compared to non-pretreated scaffold. The cell density for seeding on the scaffold was also evaluated at three different doses: 10^5, 2×10^5, and 5×10^5 per 0.005 g scaffold. In fact, the

proliferation, distribution, and differentiation of MSCs on scaffold could be affected by the cell seeding density (Zhou et al. 2011; Goldstein 2001). A previous study showed that cell-cell communication and paracrine signaling increased when cells were cultured at high density (Yassin et al. 2015).

DJ Warne et al. demonstrated that cell migration and growth were reduced by contact inhibitors in areas of high cell density. Thus, at a density of 5×10^5 cells/0.005 g scaffold, UCMSCs grew robustly during the first 7 days. However, on the 14th day of culture, the proliferation was greatly reduced and lower than that at the 3rd day. The number of cells was considerably increased from day 7 to day 14. The statistical results showed that the OD at day 14 of that density was not significantly different from the density of 5×10^5 cells/0.005 g scaffold at day 3. Therefore, at 10^5 cells and 2×10^5 cells/0.005 g scaffold densities, UCMSCs can continue to proliferate after 14 days. On the 14th day, the OD indexes of these densities were not considerable. The results suggested that the densities of 10^5cells/0.005 g scaffold could be considered as the appropriate density for further experiments.

In the next experiments, 10^5 UCMSCs/0.005 g scaffold were seeded on the pretreated scaffold after 14 days of expansion and were induced into osteoblasts in the osteogenic-inducing medium. After the 28th day of differentiation, UCMSCs clearly condensed to form clusters of cells found on the scaffold. Indeed, the condensation was considered as a prediction of early bone morphology. When mesenchymal cells differentiate into osteoblasts, these cells experience two main events, such as condensation and recruitment of other osteoblasts (Hall and Miyake 2000; Huycke et al. 2012). Initiation of the condensation was a result of three processes, including the enhancement of mitotic activity, aggregation, and failure of a cell growth at the center (Hall and Miyake 2000).

To confirm that these UCMSCs on the scaffolds were successfully differentiated to osteoblasts, these complexes of UCMSCs and scaffold were stained with Alizarin Red to detect the accumulation of calcium. The results confirmed that differentiated UCMSCs on the scaffold successfully accumulated calcium compared to the control (undifferentiated). Moreover, these differentiated UCMSCs expressed osteoblast-specific genes, including *runx2*, *OCN*, and *OPN*. During the osteogenic differentiation, *runx2* plays an important role in osteogenic differentiation of mesenchymal stem cells to the osteoblast and is express in the early stages of osteoblast differentiation (Jafary et al. 2017). Hence, the *runx2* expression has to be downregulated in the late stage of the osteogenic differentiation in the mature osteoblasts.

OCN is the most characteristic non-collagen protein of the osteoblasts, which expresses the cellular limitation of mineralized tissues, such as the bone extracellular matrix, the odontoblast cell, the cemented matrix, and cartilage cell hypertrophy (Sloan 2015). The expression of *OCN* was only found in the osteoblast (Wei and Karsenty 2015). Therefore, *OCN* is widely used as a cellular marker for osteoblast.

Moreover, the high expression of *OPN* was known as a marker of mature osteoblast. These genes were regulated by *runx2* gene via binding to the promoter of them (Ducy et al. 1997; Lian et al. 1998). In another study by Bruderer et al. (2014), the authors indicated that *runx2* helps to maintain the expression of *OPN* (Bruderer et al. 2014). This explains the relation of these genes in our research study. In the study by Huycke et al. (2012), the process of osteogenic differentiation included three steps: proliferation, transition, and maturation. In each step, the gene expression was different from each other. This was shown in our study and the research of Ding H et al. (2014). Notably, the low expression of *runx2* on day 14 was explanted by induction of the cells in the transition step (Huycke et al. 2012; Kong and Hinds 2012). When comparing it with the study of Huang et al. (2007), the enhancement of all genes demonstrated that UCMSCs could differentiate into mature osteoblasts on day 21 (Huang et al. 2007).

5 Conclusion

This study demonstrated that UCMSCs could adhere, proliferate, and differentiate on the porous scaffold to osteoblasts. At the density of 10^5cells/ 0.005 g of scaffold, the UCMSCs proliferated well on the scaffold (during day 1–14 of seeding). Furthermore, these cells at 14 days could be successfully differentiated into osteoblasts, which exhibited particular morphology and accumulated extracellular calcium expressed in the osteoblast-specific genes (*runx2*, *OPN*, and *OCN* after induction in the osteogenic medium for 21 days). These results suggested that in vitro-engineered bone tissue can be produced by UCMSCs and porous scaffold (Variotis scaffold).

Acknowledgment This research is funded by the National University Ho Chi Minh City (VNU-HCM) under grant number NV2018-18-2.

Competing Interests The authors declare that they have no conflicts of interest.

References

Ahmadi, M., Seyedjafari, E., Zargar, S. J., Birhanu, G., Zandi-Karimi, A., Beiki, B., & Tuzlakoglu, K. (2017). Osteogenic differentiation of mesenchymal stem cells cultured on PLLA scaffold coated with Wharton's Jelly. *EXCLI Journal, 16*, 785–794.

Amini, A. R., Laurencin, C. T., & Nukavarapu, S. P. (2012). Bone tissue engineering: Recent advances and challenges. *Critical Reviews in Biomedical Engineering, 40*(5), 363–408.

Aravamudhan, A., Ramos, D. M., Nip, J., Harmon, M. D., James, R., Deng, M., Laurencin, C. T., Yu, X., & Kumbar, S. G. (2013). Cellulose and collagen derived micro-nano structured scaffolds for bone tissue engineering. *Journal of Biomedical Nanotechnology, 9*(4), 719–731.

Ark, M., Boughton, P., Lauto, A., Tran, G. T., Chen, Y., Cosman, P. H., & Dunstan, C. R. (2016). Characterisation of a novel light activated adhesive scaffold: Potential for device attachment. *Journal of the Mechanical Behavior of Biomedical Materials, 62* (Supplement C), 433–445.

Bruderer, M., Richards, R., Alini, M., & Stoddart, M. (2014). Role and regulation of RUNX2 in osteogenesis. *European Cells & Materials, 28*(28), 269–286.

Chen, W., Liu, J., Manuchehrabadi, N., Weir, M. D., Zhu, Z., & Xu, H. H. (2013). Umbilical cord and bone marrow mesenchymal stem cell seeding on macroporous calcium phosphate for bone regeneration in rat cranial defects. *Biomaterials, 34*(38), 9917–9925.

Cooper, G. M. (2000). Cell proliferation in development and differentiation. In *The cell: A molecular approach* (2nd ed.). Sunderland: Sinauer Associates.

Costa-Pinto, A. R., Reis, R. L., & Neves, N. M. (2011). Scaffolds based bone tissue engineering: The role of chitosan. *Tissue Engineering Part B, Reviews, 17*(5), 331–347.

David, J., Magee, J. E. Z., & Quillen, W. S. (2007). *Scientific foundations and principles of practice in musculoskeletal rehabilitation*. In Musculoskeletal Rehabilitation Series (MRS), Chapter 1 (pp. 1–22). Missouri: Saunders Elsevier.

Ding, H., Chen, S., Yin, J. H., Xie, X. T., Zhu, Z. H., Gao, Y. S., & Zhang, C. Q. (2014). Continuous hypoxia regulates the osteogenic potential of mesenchymal stem cells in a time-dependent manner. *Molecular Medicine Reports, 10*(4), 2184–2190.

Dominici, M., Le Blanc, K., Mueller, I., Slaper-Cortenbach, I., Marini, F., Krause, D., Deans, R., Keating, A., Prockop, D., & Horwitz, E. (2006). Minimal criteria for defining multipotent mesenchymal stromal cells. The International Society for Cellular Therapy position statement. *Cytotherapy, 8*(4), 315–317.

Ducy, P., Zhang, R., Geoffroy, V., Ridall, A. L., & Karsenty, G. (1997). Osf2/Cbfa1: A transcriptional activator of osteoblast differentiation. *Cell, 89*(5), 747–754.

Fakhry, M., Hamade, E., Badran, B., Buchet, R., & Magne, D. (2013). Molecular mechanisms of mesenchymal stem cell differentiation towards osteoblasts. *World Journal of Stem Cells, 5*(4), 136–148.

Goldstein, A. S. (2001). Effect of seeding osteoprogenitor cells as dense clusters on cell growth and differentiation. *Tissue Engineering, 7*(6), 817–827.

Hall, B. K., & Miyake, T. (2000). All for one and one for all: Condensations and the initiation of skeletal development. *BioEssays, 22*(2), 138–147.

Holzmann, P., Niculescu-Morzsa, E., Zwickl, H., Halbwirth, F., Pichler, M., Matzner, M., Gottsauner-Wolf, F., & Nehrer, S. (2010). Investigation of bone allografts representing different steps of the bone bank procedure via the CAM-model. *ALTEX-Alternatives to Animal Experimentation, 27*(2), 97–103.

Huang, W., Yang, S., Shao, J., & Li, Y.-P. (2007). Signaling and transcriptional regulation in osteoblast commitment and differentiation. *Frontiers in Bioscience: a Journal and Virtual Library, 12*, 3068.

Huycke, T. R., Eames, B. F., & Kimmel, C. B. (2012). Hedgehog-dependent proliferation drives modular growth during morphogenesis of a dermal bone. *Development, 139*(13), 2371–2380.

Jafary, F., Hanachi, P., & Gorjipour, K. (2017). Osteoblast differentiation on collagen scaffold with immobilized alkaline phosphatase. *International Journal of Organ Transplantation Medicine, 8*(4), 195–202.

Kong, E., & Hinds, P. (2012). *The retinoblastoma protein in osteosarcomagenesis*. Rijeka: InTech.

Lian, J. B., Stein, G. S., Stewart, C., Puchacz, E., Mackowiak, S., Aronow, M., Von Deck, M., & Shalhoub, V. (1989). Osteocalcin: Characterization and regulated expression of the rat gene. *Connective Tissue Research, 21*(1–4), 61–68. discussion 69.

Lian, J. B., Stein, G. S., Stein, J. L., & van Wijnen, A. J. (1998). Osteocalcin gene promoter: Unlocking the secrets for regulation of osteoblast growth and differentiation. *Journal of Cellular Biochemistry. Supplement, 30–31*, 62–72.

McKee, M. D., & Nanci, A. (1996). Osteopontin: An interfacial extracellular matrix protein in mineralized tissues. *Connective Tissue Research, 35*(1–4), 197–205.

Mishra, R., Bishop, T., Valerio, I. L., Fisher, J. P., & Dean, D. (2016). The potential impact of bone tissue engineering in the clinic. *Regenerative Medicine, 11*(6), 571–587.

Oldberg, A., Franzén, A., & Heinegård, D. (1986). Cloning and sequence analysis of rat bone sialoprotein (osteopontin) cDNA reveals an Arg-Gly-Asp cell-binding sequence. *Proceedings of the National Academy of Sciences, 83*(23), 8819–8823.

Pavasant, P., Shizari, T. M., & Underhill, C. B. (1994). Distribution of hyaluronan in the epiphysial growth plate: Turnover by CD44-expressing osteoprogenitor cells. *Journal of Cell Science, 107*(Pt 10), 2669–2677.

Roach, H. (1994). Why does bone matrix contain non-collagenous proteins? The possible roles of osteocalcin, osteonectin, osteopontin and bone sialoprotein in bone mineralisation and resorption. *Cell Biology International, 18*(6), 617–628.

Robling, A. G., Castillo, A. B., & Turner, C. H. (2006). Biomechanical and molecular regulation of bone remodeling. *Annual Review of Biomedical Engineering, 8*, 455–498.

Rutkovskiy, A., Stensløkken, K.-O., & Vaage, I. J. (2016). Osteoblast differentiation at a glance. *Medical Science Monitor Basic Research, 22*, 95–106.

Sloan, A. J. (2015). Chapter 29: Biology of the dentin-pulp complex. In A. Vishwakarma, P. Sharpe, S. Shi, & M. Ramalingam (Eds.), *Stem cell biology and tissue engineering in dental sciences* (pp. 371–378). Boston: Academic.

Van Pham, P., Truong, N. C., Le, P. T.-B., Tran, T. D.-X., Vu, N. B., Bui, K. H.-T., & Phan, N. K. (2016). Isolation and proliferation of umbilical cord tissue derived mesenchymal stem cells for clinical applications. *Cell and Tissue Banking, 17*(2), 289–302.

Vepari, C., & Kaplan, D. L. (2007). Silk as a biomaterial. *Progress in Polymer Science, 32*(8–9), 991–1007.

Wang, L., Singh, M., Bonewald, L., & S Detamore, M. (2009). Signaling strategies for osteogenic differentiation of human umbilical cord mesenchymal stromal cells for 3D bone tissue engineering. *Journal of Tissue Engineering and Regenerative Medicine, 3*, 398–404.

Wang, L., Dormer, N. H., Bonewald, L. F., & Detamore, M. S. (2010). Osteogenic differentiation of human umbilical cord mesenchymal stromal cells in polyglycolic acid scaffolds. *Tissue Engineering Part A, 16*(6), 1937–1948.

Wang, P., Zhao, L., Liu, J., Weir, M. D., Zhou, X., & Xu, H. H. K. (2014). Bone tissue engineering via nanostructured calcium phosphate biomaterials and stem cells. *Bone Research, 2*, 14017.

Wei, J., & Karsenty, G. (2015). An overview of the metabolic functions of osteocalcin. *Reviews in Endocrine & Metabolic Disorders, 16*(2), 93–98.

Yassin, M. A., Leknes, K. N., Pedersen, T. O., Xing, Z., Sun, Y., Lie, S. A., Finne-Wistrand, A., & Mustafa, K. (2015). Cell seeding density is a critical determinant for copolymer scaffolds-induced bone regeneration. *Journal of Biomedical Materials Research Part A, 103*(11), 3649–3658.

Zhang, M., Boughton, P., Rose, B., Lee, C. S., & Hong, A. M. (2013). The use of porous scaffold as a tumor model. *International Journal of Biomaterials, 2013*, 396056.

Zhang, M., Rose, B., Lee, C. S., & Hong, A. M. (2015). In vitro 3-dimensional tumor model for radiosensitivity of HPV positive OSCC cell lines. *Cancer Biology & Therapy, 16*(8), 1231–1240.

Zhou, H., Weir, M. D., & Xu, H. H. (2011). Effect of cell seeding density on proliferation and osteodifferentiation of umbilical cord stem cells on calcium phosphate cement-fiber scaffold. *Tissue Engineering Part A, 17*(21–22), 2603–2613.

Ziros, P. G., Basdra, E. K., & Papavassiliou, A. G. (2008). Runx2: Of bone and stretch. *The International Journal of Biochemistry & Cell Biology, 40*(9), 1659–1663.